The role of myosin phosphorylation in anaphase chromosome movement

Rozhan Sheykhani[1], Purnata V. Shirodkar[1], Arthur Forer[1*]

[1] Department of Biology, York University, Toronto, Ontario, Canada M3J 1P3

[*] Corresponding author

aforer@yorku.ca
+1- 416-736-5398

Abstract

This work deals with the role of myosin phosphorylation in anaphase chromosome movement. Y27632 and ML7 block two different pathways for phosphorylation of the myosin regulatory light chain (MRLC). Both stopped or slowed chromosome movement when added to anaphase crane-fly spermatocytes. To confirm that the effects of the pharmacological agents were on the presumed targets, we studied cells stained with antibodies against mono- or bi-phosphorylated myosin. For all chromosomes whose movements were affected by a drug, the corresponding spindle fibres of the affected chromosomes had reduced levels of 1P- and 2P-myosin. Thus the drugs acted on the presumed target and myosin phosphorylation is involved in anaphase force production.

Calyculin A, an inhibitor of MRLC dephosphorylation, reversed and accelerated the altered movements caused by Y27632 and ML-7, suggesting that another phosphorylation pathway is involved in phosphorylation of spindle myosin. Staurosporine, a more general phosphorylation inhibitor, also reduced the levels of MRLC phosphorylation and caused anaphase chromosomes to stop or slow. The effects of staurosporine on chromosome movements were not reversed by Calyculin A, confirming that another phosphorylation pathway is involved in phosphorylation of spindle myosin.

Keywords: phosphorylated myosin, spindle fibre, chromosome movement, crane-fly spermatocyte, kinase inhibitor, calyculin A.

Introduction

Chromosome movement during anaphase has long been studied but the exact roles of the different cytoskeleton elements still are not resolved. Most hypotheses of force production focus solely on spindle microtubules and their motor proteins (Gorbsky et al., 1988; Nicklas, 1989; Desai et al., 1998; Sharp et el., 2000; LaFountain et al., 2004; Mitchison, 2005; Rogers et al., 2005; Rath et al., 2009). Others have considered components such as actin (Forer and Pickett-Heaps, 1998; Silverman-Gavrila and Forer, 2000; Forer, et al., 2003; Robinson and Snyder, 2003; Fabian and Forer, 2005 and 2007; Snyder et al., 2010), myosin (Fabian and Forer; 2005, 2007; Fabian et al., 2007; Silverman-Gavrila and Forer, 2000, 2003; Rosenblatt et al., 2004; Woolner et al., 2008; Snyder et al., 2010; Rump et al., 2011), titin (Fabian et al., 2007) and spindle matrix proteins (Johansen and Johansen, 2007; Lince-Faria et al., 2009; Qi et al., 2009; Ding et al., 2009; Johansen et al., 2011). This article describes experiments that deal with the role of spindle myosin in anaphase chromosome movement.

Myosin interacts with microtubules in various cytoskeleton systems in a variety of organisms [reviewed by Rodriguez et al. (2003)]. For spindles in particular, myosin is present in a broad range of spindles, as is actin (Forer et al., 2003). Functionally, in *Xenopus laevis* embryos unconventional myosin-10 associates with spindle microtubules and integrates F-actin and microtubules to maintain spindle length and mitosis progression (Weber et al., 2004; Woolner et al., 2008). In *Drosophila* spindles, unconventional myosin-6 binds to CLIP-190 and thereby indirectly crosslinks actin and microtubules (Lantz and Miller, 1998). In cardiac myocytes, ablation of non-muscle myosin II-B and II-C causes major defects in karyokinesis (Ma et al., 2010). In *Dictyostelium discoideum* myosin-1C is associated with both spindle microtubules and F-actin and plays an important role in maintaining spindle stability and

chromosome segregation (Rump et al., 2011). In crane-fly spermatocytes, immunostaining and pharmacological evidence show that myosin is present in spindle fibres and is involved in poleward chromosome movements and flux (Silverman-Gavrila and Forer, 2001; Fabian and Forer, 2005; Fabian et al., 2007).

Myosin regulation occurs in many systems via phosphorylation of the myosin regulatory light chain (MRLC), which activates the myosin (Sellers, 1991; Trybus, 1991; Komatsu et al., 2000). There are two major sites for MRLC phosphorylation: the primary (more preferred) serine 19 site and the secondary threonine 18 site, which are phosphorylated separately. MRLC also can be biphosphorylated on both sites (Ikebe and Hartshorne, 1985; Tan et al., 1992). Phosphorylation of MRLC on the Thr18/Ser19 sites arises from various kinases including Rho-kinase (ROCK), myosin light chain kinase (MLCK), Citron kinase, etc., and these enzymes work differently in mono- or di-phosphorylation of MRLC of various cells (Haeberle, 1988; Amano et al., 1996; Sakurada et al., 1998; Cremo and Hartshorne, 2008). Dephosphorylation of MRLC, on the other hand, is due to a single enzyme, myosin light chain phosphatase (MLCPase), of the class protein phosphatase 1. MRLC dephosphorylation causes myosin inactivation (Brozovich, 2002) and blocking dephosphorylation enhances myosin activity. For example, blocking MLCPase using Calyculin A (CalA) blocks dephosphorylation of MRLC, and the resultant hyper-phosphorylated myosin causes increased contraction in rabbit smooth muscle (Suzuki and Itoh, 1993). With respect to spindle myosin phosphorylation, spindle MLCK has been detected by antibody staining and by studying labeled protein in vivo (Guerriero et al., 1981; Poperechnaya et al., 2000; Dulyaninova et al. 2004). Genetically engineered MLCK alterations cause changes in mitosis further implicating myosin in mitotic force mechanisms (Komatsu, 2000; Dulyaninova et al. 2004). CalA causes accelerated chromosome movement towards the

pole in crane fly spermatocytes, most likely due to hyper-activation of myosin (Fabian et al., 2007). Blocking MRLC phosphorylation in PtK2 cells with Y-27632, which inhibits ROCK, interferes with spindle assembly and centrosome positioning (Rosenblatt et al., 2004). Y-27632 temporarily slowed or stopped chromosome movement in crane-fly spermatocytes, from which Fabian and Forer (2007) concluded that the ROCK pathway phosphorylates spindle fibre MRLC. Because Y-27632 blocks myosin phosphorylation, the treated myosin would not be phosphorylated, so the effects of Y-27632 should not be reversed by CalA. But CalA *did* cause acceleration of anaphase movements in cells treated with Y-27632. Therefore, Fabian and Forer (2007) hypothesized that spindle myosin can be phosphorylated by additional pathways.

In this article we used inhibitors to test the role of myosin-phosphorylation in anaphase. We added different inhibitors to anaphase cells, separately or together, and followed subsequent chromosome movement; we tested whether the inhibitors acted on the presumed target (spindle myosin) by quantifying the staining intensities of phosphorylated spindle myosin before and after drug treatment. The data show that the drugs indeed reduce spindle myosin phosphorylation, and that spindle myosin phosphorylation can occur via redundant pathways.

Materials and methods:

Living cell preparations and cell treatment

We followed the protocol for preparing living crane-fly (*Nephrotoma suturalis* Loew) spermatocytes described by Forer and Pickett-Heaps (1998, 2005). Briefly, we dissected testes from 4th instar larvae under Halocarbon oil 200 (Halocarbon Products Corp., N.Y., U.S.A) and rinsed them three times with insect Ringer's solution: 0.13 M NaCl, 5 mM KCl, 1 mM CaCl2, 0.02 M Na2HPO4–KH2PO4 buffer (pH 6.9). We placed one testis on a glass coverslip in

Ringers solution containing fibrinogen (Calbiochem), pierced it, and shortly after added thrombin (Sigma) to form a fibrin clot. The coverslip with cells then was attached to a perfusion chamber and perfused with insect Ringers solution. As the cells were observed using phase-contrast microscopy the cells were perfused with insect Ringers solution containing the drug in question. When the purpose of experiment was to quantify the intensity of mono and bi-phosphorylated myosin using confocal microscopy, we put a dilute sample of glycerinated rabbit myofibrils (in insect Ringers solution) in the fibrinogen, so we could use staining of myofibrils as a 'standard' for quantifying phosphorylated myosin in spindles.

We used the following inhibitors at the final concentrations listed: 10 µM staurosporine (LC Laboratories), 100 µM Y-27632 ((*R*)-(+)-*trans*-N-(4-pyridyl)-4-(1-aminoethyl)-cyclohexanecarboxamide (LC Laboratories), 75 µM ML-7 (1-(5-iodonaphthalene-1-sulfonyl)-1H-hexahydro-1,4-diazepine hydrochloride) (Toronto Research Chemicals), 100 nM Calyculin A (LC Laboratories), 20 µM Bisindolylmaleimide I (BIM) (Sigma) and 20 mM 2,3-butanedione 2-monoxime (BDM) (Sigma). These drugs have been used previously in these cells at various concentrations (Silverman-Gavrila and Forer, 2001; Fabian and Forer, 2005, 2007; Fabian et al., 2007), and for the present experiments we have chosen concentrations at the higher end of their effective range. All drug stocks were stored at 1000 times the concentration added to the cells, all except BDM and Y-27632 were stored in dimethyl sulfoxide (DMSO), and all were diluted 1:1000 into insect Ringers solution to eliminate the adverse effect of DMSO on the cells. Control experiments have shown that 0.1% DMSO has no detectable effects on anaphase (Forer and Pickett-Heaps, 1998; Silverman-Gavrila and Forer, 2001). BDM and Y-27632 stocks were made in insect Ringers solution and diluted 1:1000 with insect Ringers solution before adding them to the cells.

Microscopy and measurements

Living cells were observed using phase-contrast microscopy with a 100X oil immersion Nikon objective, numerical aperture 1.3. We recorded images on DVD discs in real time, and then time-lapsed and converted images to avi files using Virtual Dub freeware (*www.virtualdub.org)*. Interkinetochore distances and anaphase chromosome movement velocities were measured using a program developed in the lab (Wong and Forer, 2003) and plotted using a commercial program (SlideWrite).

Fluorescent staining and confocal microscopy

We modified the staining protocol used by Fabian and Forer (2005). Treated or control crane-fly spermatocytes were lysed for 20-40 minutes in a lysis buffer (100 mM piperazineN,N-bis(2-ethanesulfonic acid) [PIPES]; 10 mM EGTA; 5 mM MgSO4; 5% DMSO; 1% Nonidet P-40; pH 6.9). Lysed cells were fixed for 6 minutes in 0.25% glutaraldehyde in phosphate-buffered saline (PBS), rinsed in PBS (two times for 5 minutes each), kept for 10 to 15 minutes in sodium borohydride (1 mg/ml) to neutralise free aldehyde groups, rinsed again with PBS (two times for 5 minutes each) and stored in PBS–glycerol 1:1 (v/v) at 4^{o}C. After removing the PBS/glycerol, cells were double stained for total MRLC-tubulin, for mono-phosphorylated MRLC-tubulin, or for bi-phosphorylated MRLC-tubulin. All staining steps were done at room temperature. Glycerol:PBS was removed prior to staining by rinsing the dishes with PBS (two times for 20 minutes each) and then, to facilitate spreading of the antibody, with PBS containing 0.1% Triton X-100 before adding the antibodies. The incubation time for each antibody was 45 minutes; after each incubation period, the cells were rinsed two times for 5 min each with PBS and then with

PBS containing 0.1% Triton X-100. Preparations were kept in the dark during the incubation periods to prevent light inactivation of the fluorochromes.

For total MRLC-tubulin staining, myosin was stained with MY-21, a mouse IgM antibody against myosin regulatory light chain (Sigma), diluted 1:100, followed by Alexa 488 Goat anti-mouse IgM (Invitrogen, Burlington, ON, Canada), diluted 1:100. Tubulin was stained with YL1/2 rat monoclonal antibody specific for tyrosinated α-tubulin diluted (1:200), followed by Alexa 594 goat anti-rat immunoglobulin IgG (Invitrogen, Burlington, ON, Canada) diluted 1:100. For 1P myosin-tubulin staining, mono phosphorylated myosin regulatory light chain was stained with Phospho-Myosin Light Chain 2 (Ser19) Mouse IgG antibody (Cell Signaling (NEB), Pickering, ON, Canada) diluted 1:150 followed by Alexa 488 Goat anti-mouse IgG, diluted 1:200. Tubulin was stained as in myosin-tubulin preparations. For 2P myosin-tubulin staining, bi-phosphorylated myosin regulatory light chain was stained with Phospho-Myosin Light Chain 2 (Thr18/Ser19) rabbit antibody (Cell Signaling (NEB), Pickering, ON, Canada) diluted 1:150 followed by Alexa 488 Goat anti-rabbit, diluted 1:200. Tubulin was stained as in myosin-tubulin preparations. All dilution of antibodies was done in PBS. Coverslips were mounted in Mowiol (Calbiochem, Billerica, MA, USA) solution (Osborn and Weber, 1982) containing paraphenylene diamine (PPD) as antifading agent (Fabian and Forer, 2005), and stored at 4^{o}C in the dark.

When we studied single cells previously followed using light microscopy, we needed to remove antibodies from a cell that was stained previously with 1P-myosin antibody and stain the same cell for a second time with 2P-myosin antibody. In order to do this, we followed and optimized the protocol suggested by Legocki and Verma (1981). To remove the mowiol and release the coverslip from the slide we immersed the slide in PBS plus 0.1% triton (or NP40)

overnight. After removing the coverslip from the slide we rinsed the cells in PBS twice, and then we immersed the cells for 2-5 minutes in a buffer containing 20 mM $MgAc_2$, 30 mM KCl, 0.1 M glycine-HCl (pH 2.2). This was followed by twice rinsing in PBS. We viewed them in the confocal microscope to verify that this treatment removed all previous antibodies, and we subsequently followed the staining procedures given above. There often was increased 'autofluorescence' of chromosomes after removal of the first antibodies, however.

Stained cells were studied using an Olympus Fluoview 300 confocal microscope with argon laser at 488 nm and HeNe laser at 543 nm and 660 nm, using an Olympus Plan Apo 60X oil immersion objective (numerical aperture, 1.4). Images, collected with Fluoview software, were further processed using Image J and Adobe Photoshop.

To quantify the amount of phosphorylated myosin in spindle fibres, we used Image J freeware. Using Image J we drew a line in the background and a line along the spindle fibres of the chosen cell and obtained grey scale values representing p-myosin intensity at each pixel along the line (Fig. 1A). As shown previously by Fabian et al. (2007), in their Figure 5, the staining of P-myosin was punctate, which produced peaks in the grey value graph vs. distance. For analysis we took the average intensities of all the pixels in the spindle fibre, subtracted average background intensities obtained from a scan of a similar line outside the cells, and obtained a single number for the average intensity of that fibre. Since staining results often vary between different slides prepared on the same day, let alone prepared on different days, we used staining of glycerinated myofibrils near the cells in question as 'standards', since they would not be affected by any of the treatments and the amounts of the myosin in question should be the same in different myofibrils: we measured the intensities of pixels along stained (myosin-containing) areas of myofibrils (Fig. 1B), obtained average intensities, subtracted background

staining intensities, and adjusted the grey scale levels of the spindle fibre staining based on the average staining intensities of the nearby myofibrils on the same slides. For example, if a control cell had a spindle fibre average intensity of 900 and the myofibril 2000 and an experimental spindle fibre had an average intensity of 700 but myofibril staining of 2500, to compare the control with the experimental spindle fibre we would multiply the experimental spindle fibre average intensity (700 in this example) by 2000/2500. For all such control-control or control-experimental comparisons we adjusted the data in this way, normalising against the staining intensities in nearby myofibrils. We assessed the differences between average values using student's t-test.

Results

Pharmacological studies

Control cells:

Crane-fly spermatocytes have three bivalent autosomes and two univalent sex chromosomes (Forer, 1982). During anaphase of meiosis I, the three autosomal pairs move toward the poles with constant separation velocities ranging from 0.5 to 1.5 μm/min (Fig. 2) (Forer, 1969; Schaap and Forer, 1979 LaFountain et al., 2001). After the autosomes near the poles, the two sex chromosome univalents start their own anaphase movements from the equator to the poles with a slower velocity about 0.2 to 0.3 μm/min (Schaap and Forer, 1979). Cytokinesis starts after sex chromosome anaphase has begun.

Drug treatments

To investigate the effect of different drugs on anaphase autosome movement, we treated crane-fly primary spermatocytes with inhibitors shortly after anaphase started. The major effects after treating with inhibitors were that chromosomes stopped moving (Figs. 3B) or slowed (Fig.

4A). In cells that were affected by the drug in question not all chromosomes responded the same (Fig. 3C), but both separating (partner) chromosomes (formerly paired as bivalents) always responded the same. Sometimes poleward movements resumed in the continued presence of the drug albeit usually at reduced velocities (Fig. 4A).

To investigate whether there are redundant phosphorylation pathways, our basic protocol was first to treat cells in anaphase with different kinase inhibitors, and then, when the drug slowed or stopped poleward chromosome movement, to challenge the cells with Calyculin A (CalA) in the continued presence of the kinase inhibitors. CalA causes the acceleration of normal chromosome movement (Fig. 3A), probably due to hyperphosphorylation of myosin (Fabian et al., 2007). If there are several pathways to phosphorylate spindle myosin and the drug in question blocks them all, then CalA would not reverse the effect and chromosomes would not accelerate to the poles. However, if the drug blocks one phosphorylation pathway and there are alternate pathways, then phosphorylation still can take place and CalA would reverse the effect of the drug. Thus if there are alternate pathways, chromosome movement would stop or slow after the addition of the kinase inhibitor, and CalA (in the continued presence of the drug) would cause the stopped/slowed chromosomes to accelerate to velocities higher than those before drug treatment. We now describe the results of these experiments.

Effects of Staurosporine

Staurosporine, a *Streptomyces staurosporesa* alkaloid that blocks variousserine/threonine specific protein kinases, acts by preventing ATP binding because of its stronger affinity for the kinase (Ruegg and Burgess, 1989; Tamaoki et al., 1986; Karaman et al., 2008). When we treated crane-fly primary spermatocytes with 10 µM staurosporine in anaphase (e.g., Fig. 3B, Fig. 3C), chromosome movement stopped or slowed in 31/37 of the chromosome pairs studied (Table 1A).

Of the slowed chromosome pairs, separation velocities were on average 3.7 times slower than before 10 µM staurosporine treatment.

In order to test whether or not staurosporine blocked all myosin phosphorylation pathways, we added 100nM CalA (in the continuing presence of 10µM staurosporine). Chromosome movement was not accelerated with CalA treatment (Table 1B, Fig. 3B), indicating that staurosporine inhibits all the MRLC phosphorylation pathways.

Staurosporine is a potent inhibitor of protein kinase C (PKC), so its effects might be because it inhibits PKC rather than myosin kinases. To test this, we treated the cells with 20µM Bisindolylmaleimide I (BIM). This inhibitor selectively inhibits PKC by acting as a competitive inhibitor for its ATP binding site (Toullec et al., 1991). BIM had no effect on the 13/16 of the chromosome pairs studied (Table 2 and Fig. 4A). Therefore, the effect of staurosporine on chromosome movement is not due to its effect on PKC. In four cells that were treated with BIM followed by CalA, chromosome movement was accelerated towards the poles, confirming that PKC is not involved in this effect.

Effects of blocking Rho-kinase

Staurosporine is a broad inhibitor, so in order to determine which pathways are involved in the phosphorylation of spindle myosin we treated crane-fly primary spermatocytes with more specific inhibitors that block different kinases known to phosphorylate MRLC. Fabian and Forer (2007) showed that Y-27632, a Rho kinase inhibitor, slowed or stopped chromosome movement and this effect was reversed with the addition of CalA. We confirmed these results using 100 µM Y-27632; chromosome movement either slowed or stopped in 11/14 chromosome pairs studied (Table 3A, Fig. 4A). 100 nM CalA added in the continued presence of Y-27632 caused all affected chromosomes to accelerate towards the poles. Thus Rho-kinase seems to be involved

with phosphorylation of spindle myosin, but other pathways also seem to be involved. Some chromosome pairs that were not affected by the Y-27632 did not accelerate, however (Table 3B).

Effects of blocking MLCK

We inhibited MLCK using ML-7. This drug selectively inhibits MLCK and impairs myosin activity in different cell types by competing for the MLCK ATP-binding sites (Shoemaker et al., 1990; Lucero et al., 2006). 75 µM ML-7 added a few minutes after anaphase onset caused 18/26 half-bivalent pairs to either slow or stop (Table 4A). The velocities of the slowed down chromosomes were about 2.5 times slower than pre-treatment anaphase velocities. The effects of 75 µM ML-7 in slowing or stopping chromosomes were reversed by 100nM CalA, which caused the slowed/stopped chromosomes to accelerate (Table 4B, Fig. 5). Thus MLCK seems to be involved in myosin phosphorylation in crane-fly spermatocytes but it is not the only pathway to do so.

Effects of blocking both ROCK and MLCK

If ROCK and MLCK were the only pathways involved in MRLC phosphorylation, then CalA would not accelerate the chromosomes after double treatments of both drugs simultaneously. 75 µM ML-7 and 100 µM Y-27632 added together, a few minutes after anaphase onset, caused 14/20 of the half-bivalent pairs we followed to either slow or stop (Table 5A). On average, slowed chromosome movement after the double treatment was about 30% the speed of anaphase chromosome movement before the addition of the drugs. Addition of 100 nM CalA (in the continued presence of ML-7 and Y-27632) caused chromosome acceleration in all the chromosome pairs affected by the double treatment, but did not cause acceleration in those half-bivalent pairs not affected by the kinase inhibitors (Table 5B). These data implicate MLCK

and Rho in phosphorylation of spindle myosin but suggest that there might be yet another pathway involved in the phosphorylation of MRLC in crane-fly spermatocytes.

Immunostaining studies

1P and 2P-myosin levels in spindle fibres in drug-treated cells

We have assumed that the drug treatments alter spindle myosin phosphorylation levels. Since the treatments are global, though, potentially acting on all cell components and not just spindles, it is important to verify that the drugs indeed affected their targets (spindle myosin). We assessed this using immunofluorescence.

Immunofluorescence staining confirmed that mono- and bi-phosphorylated myosin are located in spindle fibres of crane-fly spermatocytes (Fig. 6). We quantified staining of spindle fibres and staining of nearby myofibrils. In myofibrils 2P-myosin is about 71% the intensity of 1P-myosin; in spindle fibres 2P- myosin is about 47% the intensity of 1P-myosin. We cannot say whether these differences reflect differences in affinity of the antibodies or differences in amounts of antigen, but previous reports have shown that in muscle there are higher amounts of mono-phosphorylated MRLC at Ser19 compared to bi-phosphorylation (Haberle, 1988; Sakurada, 1998). The same might apply to spindle myosins.

We quantified staining intensities of 1P- and 2P-myosin in large numbers of spindle fibres in cells in control cells and in cells treated with different drugs. We scanned individual spindle fibres, backgrounds, and nearby myofibrils, and normalised the average staining of each fibre relative to the staining of nearby myofibrils, as described in the Methods section. That allows us to compare different treatments to see if they had effects on phosphorylated spindle myosin. All three phosphorylation inhibitors (ML-7, staurosporine, Y-27632) reduced the levels of 1P- and 2P-myosin, and, except for Y27632, seemed to preferentially reduce the levels of 2P-

myosin (Fig. 7). 100 nM CalA increased the level of 2P-myosin (Fig. 8), similar to results of Sakurada et al. (1998) on effects of Cal A on 1P and 2P levels in MRLC in smooth muscle. As a control for our quantification we treated cells with BDM, which inhibits myosin ATPase (Forer and Fabian, 2005) but not its phosphorylation. BDM had no effect on the amount of 1P-myosin in the spindle fibres of treated crane-fly spermatocytes (Figure 9A).

Our staining of drug treated cells thus indicates that the drugs do indeed act on the presumed target, spindle myosin, to inhibit its phosphorylation.

The effect of staurosporine on total spindle myosin

Decreased amounts of phosphorylated myosin in spindles could be due to loss of MRLC from the spindles, or could be due to dephosphorylation of the myosin that stayed in place in the spindle fibres. To determine which occurs in crane-fly spermatocytes we quantified the total amount of MRLC in control and staurosporine treated cells. There was no difference (Fig. 9B), so the decreased levels of phosphorylation caused by staurosporine (and presumably the other inhibitors) was not due to loss of MRLC from the spindle, but rather to reduced levels of phosphorylation of a constant amount of spindle myosin.

Single cell studies

We quantified 1P- and 2P-myosin in spindles in the same single cells that we studied live during treatment with Y-27632, ML-7, or staurosporine. The results from staining random cells, described above, could be misleading because the effects of the drugs differed in different cells, and even between chromosomes in the same cell (Fig. 3C). Thus, in order to correlate directly the physiological effects of the myosin phosphorylation inhibitor and the level of mono- and bi-phosphorylated myosin, we studied phosphorylation levels of spindle fibres associated with specific chromosomes, the effects on which we knew.

We studied 15 cells, 5 treated with 10 µM staurosporine, 5 treated with 100 µM Y-27632 and 5 treated with 75 µM ML-7. Chromosome movements were altered in 4 of the cells treated with staurosporine, in 4 of the cells treated with Y-27632, and in 3 of the cells treated with ML-7. Examples of the effect of these inhibitors on chromosome movements are shown in Figures 3C, and 10 A to C. These treated cells were lysed, fixed and stained for tubulin and 1P-myosin; later the antibodies were removed and the same cells were stained with antibodies against tubulin and 2P-myosin. Illustrations of three cells we followed are given in Fig. 11. For all chromosomes whose movements were affected by the drug, the corresponding spindle fibres of the affected chromosomes had reduced 1P and 2P-myosin (Figs 12-14). For those chromosomes whose movements were not affected, however, most of the time the level of P-myosin also was reduced (Figs 12-14). We think this is because those chromosomes move poleward using alternate mechanism(s) that are independent of myosin, as we discuss below.

Discussion

The main conclusions from our experiments are that spindle myosin phosphorylation is a target of the drugs that we applied, that myosin phosphorylation is reduced whenever chromosome movement is altered by the drugs, and that there are alternate pathways to phosphorylate spindle myosin in addition to Rho kinase and myosin light chain kinase.

The amounts of both 1P- and 2P-myosin in spindle fibres were reduced by each of the inhibitors we applied, ML-7, Y-27632 and staurosporine (Fig. 7). Since phosphorylated myosin is the active form of myosin and is associated with spindle fibres (Figs. 1,6), and since inhibitors that alter chromosome movement also reduce myosin phosphorylation, these results lend strength to our conclusion that these inhibitors alter chromosome movements because they interfere with

the activity of spindle myosin. This conclusion is further strengthened by the experiments that show that CalA accelerates chromosome movement and also increases myosin phosphorylation. CalA stimulates muscle contraction by increasing MRLC phosphorylation (Burdyga et al., 2003), and in smooth muscle cells induces bi-phosphorylation of MRLC in Thr 18/Ser 19 (Sakurada et al., 1998). The same holds true for spindle myosin. While there was no statistically significant increase in 1P-myosin, CalA significantly increased the level of 2P-myosin (Fig. 8). Thus our experiments show that chromosome movements are slowed/stopped by inhibitors that reduce spindle myosin phosphorylation and are accelerated by an inhibitor that increases bi-phosphorylation of spindle myosin, strengthening the conclusion that myosin is involved with anaphase force production.

We studied individual cells where we knew the outcome for each chromosome pair in the cell: when each myosin phosphorylation inhibitor altered anaphase chromosome movement the associated spindle fibre had reduced phosphorylation (Figs. 12-14). Since the inhibitors reduced phosphorylation levels in general, and always reduced the levels of spindle fibres associated with slowed/stopped chromosomes, we conclude that spindle fibre myosin is involved with force production for anaphase chromosome movement. This conclusion is consistent with previous studies that have indicated that myosin is present in the spindle, and that inhibitors of myosin and genetic manipulation of myosin alter spindles and chromosome movements.

Myosin has been identified as a spindle component in a variety of cells (reviewed in Forer et al., 2003; Woolner and Bement, 2009; Sandquist et al., 2011) and both myosin and phosphorylated myosin are localised in spindle fibres. For example, myosin and/or P-myosin are present in human mitotic spindles (Fujiwara and Pollard, 1976), in PtK cell spindles (Sanger et al., 1989; Snyder et al., 2010), in crane-fly spermatocyte spindles (Figs. 1,6; also Siverman-

Gavrila and Forer, 2001 and 2003; Fabian et al., 2005; Fabian et al., 2007), in *Xenopus* oocyte spindles (Weber et al., 2004), and in sand-dollar spindles (Uehara et al., 2008). Spindle myosin has also been identified in vivo using fluorescently-labelled myosin (Rump et al., 2011). Thus, myosin is a component of spindle fibres and, since it is phosphorylated, spindle myosin is in an active state.

Inhibitor studies and genetic manipulations indicate that myosin functions to move chromosomes. For example, staurosporine interrupted chromosome formation at the metaphase plate in dividing cells of sea urchin eggs (Mabuchi et al., 1990). Various myosin inhibitors altered chromosome movements in crane-fly and locust spermatocytes (Siverman-Gavrila and Forer, 2001 and 2003; Fabian et al., 2005; Fabian and Forer, 2007; Fabian et al., 2007) and in PtK cells (Snyder et al., 2010). They also blocked tubulin flux along kinetochore spindle fibres in crane-fly spermatocytes (Siverman-Gavrila and Forer, 2001, Forer et al., 2007 and 2008). Microinjection of a catalytic fragment of MLCK into dividing NPK cells delayed the transition from nuclear envelope breakdown to the start of anaphase (Fishkind et al., 1991). Genetic studies have shown that an ‘unconventional’ myosin is important in spindle length control during mitosis (Woolner and Bement, 2009). Overexpression of un-phosphorylatable MRLC interfered with anaphase onset in rat cells (Komatsu et al. 2000). Genetic disruption of endogenous MLCK caused microtubule defects and resulted in metaphase chromosome alignment defects and metaphase arrest in HeLa cells (Dulyaninova et al. 2004). SiRNA-mediated knockdown and overexpression of dominant-negative myosin VI tail both inhibited myosin VI activity and caused a delay in metaphase progression and a defect in cytokinesis (Arden et al., 2007). Knockdown of unconventional myosin 10 in *Xenopus laevis* caused mitotic spindle defects (Woolner et al., 2008). Overexpression of a myosin-1C construct containing a single point

mutation in the motor domain resulted in chromosome misalignment and partially formed spindle fibres in *Dictyostelium discoideum* (Rump et al., 2011). Thus, from the data presented herein and from these previously published experiments, there is every reason to believe that myosin is involved in spindle force production.

Several aspects of our data point to the idea that there are redundant mechanisms for moving chromosomes: some mechanisms rely on myosin and others are independent of myosin. One reason for saying this is that the drugs reduced myosin phosphorylation in the associated spindle fibres yet chromosomes still moved normally (Tables 1-6; Fig. 12-14). This suggests that when myosin is active in producing force the inhibitors cause the associated chromosomes to stop moving, but when myosin is not active in producing force the chromosomes do not stop moving when the myosin associated with their spindle fibres is dephosphorylated. Further, after treatment with inhibitors, CalA caused the stopped/slowed chromosomes to accelerate but usually did not cause the unaffected chromosomes to accelerate (Tables 3B, 4B, 5B). Our interpretation is that those chromosomes unaffected by the initial inhibitor were unaffected because they used a motor system independent of myosin, e.g., using tubulin and tubulin motors (Gorbsky et al., 1987; Nicklas, 1989; Desai et al., 1998; Sharp et el., 2000; LaFountain et al., 2004; Mitchison, 2005; Rogers et al., 2005; Rath et al., 2009). They remained unaffected by the CalA because myosin was not involved. Such redundant mechanisms also would explain why sometimes chromosomes stopped moving but then resumed movement in the continued presence of the inhibitor (Fig. 4A): a new mechanism kicked in that is independent of myosin. Also, it would explain why some chromosomes stopped moving (myosin alone was involved) and some slowed down (myosin contributed to anaphase movement, in part, but a myosin-independent mechanism contributed as well).

It is not a surprise that redundant mechanisms might be involved in a process as important as cell division, but it perhaps is surprising that, at least in crane-fly spermatocytes, different mechanisms would be used by different chromosomes in the same spindle. Previous studies using this same cell have pointed to similar conclusions. Fabian et al (2005) found that actin depolymerising agents slowed/stopped chromosome movements much as we described for myosin inhibitors: not all chromosomes in the cell were affected, and slowed or stopped movements recovered somewhat in the continued presence of the actin depolymerising agents. They assumed that this was due to alternative mechanisms that were independent of actin. They tested that idea by using an actin depolymerising drug to remove F-actin from the cells shortly after the start of prometaphase. These actin-filament-free cells formed metaphase spindles an hour later, and chromosomes proceeded through a normal anaphase. This shows that when F-actin is present it can be used as part of the spindle force apparatus, but when it is absent it is replaced by something else, that there are redundant spindle mechanisms.

There seem to be redundant mechanisms as well for phosphorylation of spindle myosin. Inhibiting MLCK and ROCK phosphorylation pathways individually with ML-7 and Y27632 usually slowed/stopped chromosome movement. When we challenged the same cells with CalA in the presence of the same inhibitor(s), the slowed/stopped chromosomes accelerated (Fig. 5 and Tables 4B and 5B). This suggests that MLCK and ROCK are not the only pathways involved in phosphorylating MRLC in spindle fibres, that acceleration occurred because spindle myosin was phosphorylated through other pathways. A general kinase inhibitor, staurosporine, also slowed/stopped chromosome movement, but addition of CalA to these cells (in the continued presence of staurosporine) did not cause the affected chromosomes to accelerate. These experiments suggest that staurosporine blocked all pathways to phosphorylate myosin, and thus

that there might be a third or more pathways that cooperate with MLCK and ROCK in phosphorylating MRLC in spindle fibres, similar to alternate phosphorylation pathways in smooth muscles (Amano et al., 1996; Shabir et al., 2004). One of the candidates for this alternative pathway could be citron kinase (CK) which is known to be responsible for the final steps of cytokinesis in *Drosophila melanogaster* (Naim et al., 2004). In general, MRLC phosphorylation plays an important role in the formation and ingression of the cleavage furrow; redundant phosphorylation pathways during cytokinesis have been investigated in detail (Madaule et al., 1998; Yoshizaki et al., 2004), so it is not surprising that there would be redundant pathways for phosphorylating spindle myosin.

In sum, our data strongly suggest that myosin is involved in anaphase chromosome movement, as one of several redundant mechanisms, and that spindle myosin is phosphorylated by redundant pathways including MLCK and ROCK.

Acknowledgments

This work was supported by grants from the Canadian Natural Sciences and Engineering Council to A.F.

References

Arden S.D., Puri, C., Au, J.S., Kendrick-Jones, J., Buss, F., 2007. Myosin VI is required for targeted membrane transport during cytokinesis. Mol. Biol. Cell. 18, 4750-4761.

Amano, M., Ito, M., Kimura, K., Fukata, Y., Chihara, K., Nakano, T., Matsuura, Y., Kaibuchi, K.,1996. Phosphorylation and activation of myosin by Rho-associated kinase (Rho-kinase). J. Biol. Chem. 271, 20246-20249.

Brozovich, F.V., 2002. Myosin light chain phosphatase: it gets around. Circ. Res. 90,500-502.

Burdyga, T., Mitchell, R.W., Ragozzino, J., Ford, L.E., 2003. Force and myosin light chain phosphorylation in dog airway smooth muscle activated in different ways. Respir. Physiol. Neurobiol. 137,141–149.

Cremo, C.R., Hartshorne, D.J., 2008. Smooth-Muscle Myosin II. In: ,Coluccio, L.M. (Ed.), Myosins: A Superfamily of Molecular Motors. Springer, Dordrecht, Netherlands, Vol. 7, pp. 171–222.

Desai, A., Maddox, P.S., Mitchison, T.J. and Salmon, E.D., 1998. Anaphase A chromosome movement and poleward spindle microtubule flux occur at similar rates in Xenopus extract spindles. J. Cell Biol.141, 703-713.

Ding, Y., Yao, C., Lince-Faria, M., Rath, U., Cai, W., Maiato, H., Girton, J., Johansen, K.M., Johansen, J., 2009. Chromator is required for proper microtubule spindle formation and mitosis in Drosophila. Dev Biol. 334, 253-263.

Dulyaninova, N.G., Patskovsky, Y.V., Bresnick, A.R. 2004, The N-terminus of the long MLCK induces a disruption in normal spindle morphology and metaphase arrest. J. Cell Sci. 117, 1481-1493.

Fabian, L. and Forer, A., 2005. Redundant mechanisms for anaphase chromosome movements: Crane-fly spermatocyte spindles normally use actin filaments but also can function without them. Protoplasma. 225,169-184.

Fabian, L., Xia, X., Venkitaramani, D.V., Johansen, K.M., Johansen, J., Andrew, D.J., Forer, A., 2007. Titin in insect spermatocyte spindle fibers associates with microtubules, actin, myosin and the matrix proteins skeletor, megator and chromator. J. Cell Sci. 120, 2190-2204.

Fabian, L., Troscianczuk, J., Forer, A., 2007. Calyculin A, an enhancer of myosin, speeds up anaphase chromosome movement. BMC Cell Chromosome. 6:1.

Fabian, L., Forer, A. 2007. Possible roles of actin and myosin during anaphase chromosome movements in locust spermatocytes. Protoplasma. 231, 201-213.

Fishkind, D.J., Cao, L.G., Wang, Y.L., 1991. Microinjection of the catalytic fragment of myosin light chain kinase into dividing cells: effects on mitosis and cytokinesis. J. Cell Biol. 114, 967-975.

Forer, A., 1969. Chromosome movements during cell division. In: Lima-de-Faria, A. (Ed.). Handbook of Molecular Cytology. North-Holland Publishing Company, Amsterdam,. pp. 553–601.

Forer, A., 1982. Crane fly spermatocytes and spermatids: A system for studying cytoskeletal components. Methods Cell Biol.25, 227–252.

Forer, A. and Fabian, L., 2005. Does 2,3-butanedione monoxime inhibit nonmuscle myosin? Protoplasma. 225, 1-4.

Forer, A. and Pickett-Heaps, J. D., 1998. Cytochalasin D and latrunculin affect chromosome behaviour during meiosis in crane-fly spermatocytes. Chromosome Res. 6, 533-549.

Forer, A. and Pickett-Heaps, J., 2005. Fibrin clots keep non-adhering living cells in place on glass for perfusion or fixation. Cell Biol. International 29, 721-730.

Forer, A., Spurck, T., Pickett-Heaps, J.D. and Wilson, P.J., 2003. Structure of kinetochore fibres in crane-fly spermatocytes after irradiation with an ultraviolet microbeam: neither microtubules nor actin filaments remain in the irradiated region. Cell Motil. Cytoskeleton. 56, 173-192.

Forer, A, Pickett-Heaps, J.D., and Spurck, T., 2008. What generates flux of tubulin in kinetochore microtubules? Protoplasma. 232, 137-141.

Gorbsky, G.J., Sammak, P.J. and Borisy, G.G., 1988. Microtubule dynamics and chromosome motion visualized in living anaphase cells. J. Cell Biol. 106, 1185-1192.

Guerriero, V, Jr., Rowley, D. R., and Means, A.R. (1981). Production and characterization of an antibody to myosin light chain kinase and intracellular localization of the enzyme. Cell 27, 449-458.

Haeberle, J.R., Sutton, T.A., Trockman, B.A., 1988. Phosphorylation of two sites on smooth muscle myosin. Effects on contraction of glycerinated vascular smooth muscle. J. Biol. Chem. 263, 4424-4429.

Ikebe, M., Hartshorne, D.J., 1985. Phosphorylation of smooth muscle myosin at two distinct sites by myosin light chain kinase. J Biol Chem. 260, 10027-10031.

Johansen, K.M., Johansen, J., 2007. Cell and molecular biology of the spindle matrix. Int. Rev. Cytol. 26, 155-206.

Johansen, K.M., Forer, A., Yao, C., Girton, J., Johansen, J., 2011. Do nuclear envelope and intranuclear proteins reorganize during mitosis to form an elastic, hydrogel-like spindle matrix? Chromosome Res. 19, 345-365.

Kamm, K.E., Stull, J.T., 2001. Dedicated myosin light chain kinases with diverse cellular functions. J. Biol. Chem. 276, 4527-4530.

Karaman, M.W., Herrgard, S., Treiber, D.K., Gallant, P., Atteridge, C.E., Campbell, B.T., Chan, K.W., Ciceri, P., Davis, M.I., Edeen, P.T., Faraoni, R., Floyd, M., Hunt, J.P., Lockhart, D.J., Milanov ,Z.V., Morrison, M.J., Pallares, G., Patel, H.K., Pritchard, S., Wodicka, L.M., Zarrinkar, P.P., 2008. A quantitative analysis of kinase inhibitor selectivity. Nat. Biotechnol. 26, 127–132.

Komatsu, S. Yano, T., Shibata, M., Tuft, R. A., Ikebe, M., 2000. Effects of the Regulatory Light Chain Phosphorylation of Myosin II on Mitosis and Cytokinesis of Mammalian Cells. J. Biol. Chem. 275, 34512-34520.

LaFountain J.R, Jr., Cohan C.S., Siegel A.J., and LaFountain D.J., 2004. Direct visualization of microtubule flux during metaphase and anaphase in Crane-Fly spermatocytes. Mol. Biol. Cell. 15, 5724-5732.

Lantz, V.A., Miller, K.G., 1998. A class VI unconventional myosin is associated with a homologue of a microtubule-binding protein, cytoplasmic linker protein-170, in neurons and at the posterior pole of Drosophila embryos. J. Cell Biol. 140, 897-910.

Legocki, R.P., Verma, D.P., 1981. Multiple immunoreplica Technique: screening for specific proteins with a series of different antibodies using one polyacrylamide gel. Anal Biochem. 111, 385-392.

LaFountain JR, Jr., Oldenbourg, R., Cole, R.W., Rieder, C.L., 2001. Microtubule flux mediates poleward motion of acentric chromosome fragments during meiosis in insect spermatocytes. Mol. Biol. Cell. 12, 4054-4065.

Lince-Faria, M., Maffini, S., Orr, B., Ding, Y., Cláudia Florindo, Sunkel, C.E., Tavares, A., Johansen, J., Johansen, K.M., Maiato, H., 2009. Spatiotemporal control of mitosis by the conserved spindle matrix protein Megator. J Cell Biol.184, 647-657.

Lucero, A., Stack, C., Bresnick, A.R., Shuster, C.B., 2006. A global, myosin light chain kinase-dependent increase in myosin II contractility accompanies the metaphase-anaphase transition in sea urchin eggs. Mol. Biol. Cell. 17, 4093-4104.

Ma, X., Jana, S.S., Conti, M.A., Kawamoto, S., Claycomb, W.C., Adelstein, R.S., 2010. Ablation of nonmuscle myosin II-B and II-C reveals a role for nonmuscle myosin II in cardiac myocyte karyokinesis. Mol. Biol. Cell. 21, 3952-3962.

Mabuchi, I., Takano-Ohmuro, H., 1990. Effects of Inhibitors of Myosin Light Kinase and Other Protein Kinases on the First Cell Division of Sea Urchin Eggs. Develop. Growth & Differ., 32, 549-556.

Mitchison, T.J., 2005. Mechanism and function of poleward flux in Xenopus extract meiotic spindles. Philos Trans R Soc Lond B Biol Sci. 360, 623-629.

Madaule, P., Eda, M., Watanabe, N., Fujisawa, K., Matsuoka, T., Bito, H., Ishizaki, T., Narumiya, S., 1998. Role of citron kinase as a target of the small GTPase Rho in cytokinesis. Nature. 394, 491-494.

Narumiya, S., Ishizaki, T., Uehata, M., 2000. Use and properties of ROCKspecific inhibitor Y-27632. Methods Enzymol. 325, 273-284.

Nicklas, R.B., 1989.The motor for poleward chromosome movement in anaphase is in or near the kinetochore. J. Cell Biol. 109, 2245-2255.

Naim, V., Imarisio, S., Di Cunto, F., Gatti, M., Bonaccorsi, S., 2004. Drosophila citron kinase is required for the final steps of cytokinesis. Mol. Biol. Cell. 15, 5053-5063.

Osborn, M., Weber, K., 1982. Immunofluorescence and immunocytochemical procedures with affinity purified antibodies: tubulin-containing structures. Methods Cell Biol. 24, 97-132.

Poperechnaya, A., Varlamova, O., Lin, P-j, Stull, J. T. and Bresnick, A. R., 2000. Localization and activity of myosin light chain kinase isoforms during the cell cycle. J Cell Biol. 151, 697-707.

Qi, H., Rath, U., Wang, D., Xu, Y.-Z., Ding, Y., Zhang, W., Blacketer, M., Paddy, M., Girton, J., Johansen, J., and K. M. Johansen, 2004. Megator, an essential coiled-coil protein localizes to the putative spindle matrix during mitosis. Mol. Biol. Cell. 15, 4854-4865.

Rath, U., Rogers, G.C., Tan, D., Gomez-Ferreria, M.A., Buster, D.W., Sosa, H.J., Sharp, D.J., 2009. The Drosophila kinesin-13, KLP59D, impacts Pacman- and Flux-based chromosome movement. Mol. Biol. Cell. 20, 4696-4705.

Robinson, R.W., Snyder, J.A., 2003. Redistribution of motor proteins by Cytochalasin J treatment. Cell Biol. Int. 27, 665-673.

Rodriguez, O. C, Schaefer, A. W., Mandato, C. A., Forscher, P., Bement , W. M., Waterman-Storer, C. M., 2003. Conserved microtubule-actin interactions in cell movement and morphogenesis. Nat Cell Biol. 7, 599-609.

Rogers, G.C., Rogers, S.L., Sharp, D.J., 2005. Spindle microtubules in flux. J Cell Sci. 118, 1105-1116.

Rosenblatt, J., Cramer, L. P., Baum, B., McGee, K. M., 2004. Myosin II-dependent cortical movement is required for centrosome separation and positioning during mitotic spindle assembly. Cell. 117, 361-372.

Rüegg, U.T., Burgess, G.M., 1989. Staurosporine, K-252 and UCN-01: potent but nonspecific inhibitors of protein kinases. Trends Pharmacol. Sci. 10, 218-220.

Rump, A., Scholz, T., Thiel, C., Hartmann, F. K., Uta, P., Hinrichs, M. H., Taft, M. H., Tsiavaliaris, G., 2011. Myosin-1C associates with microtubules and stabilizes the mitotic spindle during cell division. J Cell Sci. 124, 2521-2528.

Sakurada, K., Seto, M., Sasaki, Y., 1998. Dynamics of myosin light chain phosphorylation at Ser19 and Thr18/Ser19 in smooth muscle cells in culture. Am. J. Physiol. 274,1563-1572.

Sandquist, J. C., Kita, A. M., Bement, W. M., 2011. And the dead shall rise: actin and myosin return to the spindle. Dev. Cell. 21, 410-419.

Sanger, J. M., Mittal, B., Dome, J. S. and Sanger, J. W., 1989. Analysis of cell division using fluorescently labeled actin and myosin in living PtK2 cells. Cell Motil. Cytoskeleton. 14, 201-219.

Schaap, C.J., Forer, A., 1979. Temperature effects on anaphase chromosome movement in the spermatocytes of two species of crane flies (Nephrotoma suturalis Loew and Nephrotoma ferruginea Fabricius). J Cell Sci. 39, 29-52.

Sellers, J.R., 1991. Regulation of cytoplasmic and smooth muscle myosin. Curr. Opin. Cell Biol. 3, 98-104.

Shabir, S., Borisova, L., Wray, S., Burdyga, T., 2004. Rho-kinase inhibition and electromechanical coupling in rat and guinea-pig ureter smooth muscle: Ca2+-dependent and -independent mechanisms. J. Physiol. 560, 839-855.

Sharp, D.J., Rogers, G.C. and Scholey, J.M., 2000. Cytoplasmic dynein is required for poleward chromosome movement during mitosis in Drosophila embryos. Nat. Cell Biol. 2, 922-930.

Shoemaker, M.O., Lau, W., Shattuck, R.L., Kwiatkowski, A.P, Matrisian, P.E., Guerra-Santos, L., Wilson, E., Lukas, T.J., Van Eldik, L.J., Watterson, D.M., 1990. Use of DNA sequence and mutant analyses and antisense oligodeoxynucleotides to examine the molecular basis of nonmuscle myosin light chain kinase autoinhibition, calmodulin recognition, and activity. J. Cell Biol. 111,1107-1125.

Silverman-Gavrila, R.V. and Forer, A., 2000. Evidence that actin and myosin are involved In the poleward flux of tubulin in metaphase kinetochore microtubules of crane-fly spermatocytes. J. Cell Sci. 113, 597-609.

Silverman-Gavrila. R.V., Forer, A., 2001. Effects of anti-myosin drugs on anaphase chromosome movement and cytokinesis in crane-fly primary spermatocytes. Cell Motil. Cytoskeleton. 50, 180-197.

Silverman-Gavrila, R. V. , Forer, A., 2003. Myosin localization during meiosis I of crane-fly spermatocytes gives indications about its role in division. Cell Motil. Cytoskeleton. 55, 97-113.

Snyder, J. A., Ha, Y., Olsofka, C.,Wahdan, R., 2010. Both actin and myosin inhibitors affect spindle architecture in PtK1 cells: does an actomyosin system contribute to mitotic spindle forces by regulating attachment and movements of chromosomes in mammalian cells? Protoplasma. 240, 57-68.

Suzuki, A., Itoh, T., 1993. Effects of calyculin A on tension and myosin phosphorylation in skinned smooth muscle of the rabbit mesenteric artery. Br. J. Pharmacol. 109, 703-712.

Tamaoki, T., Nomoto, H., Takahashi, I., Kato, Y., Morimoto, M., Tomita, F., 1986. Staurosporine, a potent inhibitor of phospholipid/Ca++dependent protein kinase. Biochem. Biophys. Res. Commun. 135, 397–402.

Tan, J.L., Ravid, S., Spudich, J.A., 1992. Control of nonmuscle myosins by phosphorylation. Annu. Rev. Biochem. 61, 721-759.

Trybus, K.M., 1991. Regulation of Smooth Muscle Myosin. Cell Motil. Cytoskeleton. 18, 81-85.

Toullec, D., Pianetti, P., Coste, H., Bellevergue, P., Grand-Perret, T., Ajakane, M., Baudet, V., Boissin, P., Boursier, E., Loriolle, F., 1991. The bisindolylmaleimide GF 109203X is a potent and selective inhibitor of protein kinase C. J. Biol. Chem. 266, 15771 – 15781.

Uehara, R., Hosoya, H., Mabuchi, I., 2008. In vivo phosphorylation of regulatory light chain of myosin II in sea urchin eggs and its role in controlling myosin localization and function during cytokinesis. Cell Motil. Cytoskeleton. 65, 100-115.

Weber, K. L., Sokac, A. M., Berg, J. S., Cheney, R. E., Bement, W. M., 2004. A microtubule-binding myosin required for nuclear anchoring and spindle assembly. Nature. 431, 325-429.

Wong, R., Forer, A., 2003. “Signalling” between chromosomes in crane-fly spermatocytes studies using ultraviolet microbeam irradiation. Chromosome Res. 11, 771-786.

Woolner, S., O'Brien, L. L., Wiese, C., Bement, W. M., 2008. Myosin-10 and actin filaments are essential for mitotic spindle function. J Cell Biol. 182, 77-88.

Woolner, S., Bement, W. M., 2009. Unconventional myosins acting unconventionally. Trends Cell Biol. 19, 245-252.

Yoshizaki, H., Ohba, Y., Parrini, M.C., Dulyaninova, N.G., Bresnick, A.R., Mochizuki ,N., Matsuda , M., 2004. Cell type-specific regulation of RhoA activity during cytokinesis. J. Biol. Chem. 279, 44756-44762.

Table legends:

Table 1- A: Effect of 10 µM staurosporine on anaphase chromosome movement. **B:** Effect of 10 µM staurosporine and 100 nM CalA on anaphase chromosome movement.

Table 2: Effect of 20 µM BIM on anaphase chromosome movement.

Table 3- A: Effect of 100 µM Y-27632 on anaphase chromosome movement. **B:** Effect of 100 µM Y-27632 and 100 nM CalA on anaphase chromosome movement.

Table 4- A: Effect of 75 µM ML-7 on anaphase chromosome movement. **B:** Effect of 75 µM ML-7 and 100 nM CalA on anaphase chromosome movement.

Table 5- A: Effects on anaphase chromosome movement of simultaneous addition of 75 µM ML-7 and 100 µM Y-27632. **B:** Effects of 100 nM CalA following simultaneous treatment with 75 µM ML-7 and 100 µM Y-27632 on anaphase chromosome movement.

Figure legends:

Figure 1- A: Confocal image of an anaphase control cell stained with mono-phosphorylated myosin antibody (on left) and relevant quantification scan (on the right). Chromosome staining is "autofluorescence" that we have not been able to control. **B:** Confocal image of a myofibril stained with mono-phosphorylated myosin antibody (on left) and relevant quantification scan (on the right).

Figure 2: Illustrating anaphase movement of one pair of chromosomes in one of the many control cells we studied. Plot of distance between partner chromosomes (ordinate) versus time (abscissa). The dashed line represents the line of best fit through the indicated points.

Figure 3- A: : Plots of chromosome separation versus time for one pair of separating half-bivalents in a cell treated with 100 nM CalA during anaphase, illustrating one pair that the half-bivalents (circles) accelerated after the treatment and started to move backward. The dashed line (before the treatment) and solid line (after the treatment) represent the lines of best fit through the indicated points. **B:** Plots of chromosome separation versus time for one pair of separating half bivalents in a cell treated with 10 μM staurosporine during anaphase (left arrow) and few minutes later treated with 100 nM CalA in the presence of staurosporine (right arrow), illustrating one pair of half-bivalents (circles) that almost stopped after addition of staurosporine and did not accelerate after CalA. The dashed line (before the addition of staurosporine) and solid line (after addition of staurosporine which remains the same after adding CalA) represent the lines of best fit through the indicated points. **C:** shows chromosome separation vs. time of two half-bivalent pairs during anaphase in a staurosporine-treated single cell. The first arrow on the left represents the time of the addition of the inhibitor and the second arrow on the right

shows the time of lysing and fixing the cells for staining. The dashed line (before treatment) and solid line (after treatment) represent the lines of best fit through the indicated points for the affected pair (circles). The dotted line represents the line of best fit through the indicated points for the unaffected pair (triangles).

Figure 4- A: Plots of chromosome separation versus time for one pair of separating half-bivalents in a cell treated with 20µM BIM shortly after anaphase, illustrating one pair of half-bivalents (circles) that was not affected by the BIM. **B:** Plots of chromosome separation versus time for one pair of separating half-bivalents in a cell treated with100 µM Y-27632 during anaphase, illustrating one pair of half-bivalent (circles) that slowed after the addition of Y-27632 and resumed its movement with slower velocity than before the addition of the drug. The dashed line (before the addition of Y-27632), solid line (after addition of Y-27632) and dotted line (after the movement recovered) represent the lines of best fit through the indicated points.

Figure 5: Plots of chromosome separation versus time for one pair of separating half-bivalents in a cell treated with 75 µM ML-7 during anaphase (left arrow) and few minutes later treated with 100 nM CalA in the presence of ML-7 (right arrow), illustrating one pair of half-bivalent (circles) that slowed after addition of ML-7 and accelerated after CalA. The dashed line (before the addition of ML-7), solid line (after addition of ML-7) and dotted line (after addition of CalA) represent the lines of best fit through the indicated points.

Figure 6: Crane-fly spermatocytes stained with tubulin and phosphorylated myosin antibodies. First row: stained for mono-phosphorylated myosin; second row: stained for bi-phosphorylated myosin. As verified by experiments in which we switched channels, and studied non-stained

specimens, the chromosome staining for phosphorylated myosin seen here and in other images is due to “autofluorescence” that we have not been able to control.

Figure 7: Intensities of 1P-myosin and 2P-myosin in spindle fibres divided by intensities in corresponding control cells for different inhibitors. These values were normalized against nearby myofibrils and were obtained from random cells in treated preparations. The “n” values represent the number of spindle fibres that were studied.

Figure 8: 1P and 2P-myosin intensity in random cells treated with CalA vs. control cells. These values were normalized against nearby myofibrils and were obtained from random cells in control and CalA treated preparations. . The “n” values represent the number of spindle fibres that were studied. We assessed differences between average values using student’s t-test.:

*: $P \leq 0.05$)

Figure 9: A: Mono-phosphorylated myosin intensity in BDM treated cells vs. control cells. These values were normalized against nearby myofibrils and were obtained from random cells in control and BDM treated preparations. **B:** Total MRLC intensity in staurosporine treated cells vs. control cells. These values were normalized against nearby myofibrils and were obtained from random cells in control and staurosporine treated preparations. . The “n” values represent the number of spindle fibres that were studied. We assessed differences between average values using student’s t-test.

Figure 10: Chromosome separation vs. time of one separating half-bivalent pair during anaphase, (**A)** in a control cell, **(B**) in a cell treated with Y-27632 and **(C)** in a cell treated with ML-7. The first arrows on the left (in B and C) represent the time of the addition of the inhibitor and the second arrow on the right shows the time of lysing and fixing the cells for staining. The

dashed line (before treatment) and solid line (after treatment) represent the lines of best fit through the indicated points.

Figure 11: Confocal images of control, staurosporine, Y-27632 and ML-7 treated cells stained for 1P-myosin (left column) and 2P-myosin (right column). Chromosome staining is due to "autofluorescence" that we have not been able to control. Scale bar = 5μm.

Figure 12: 1P (A) and 2P (B) myosin intensity in single cells treated with staurosporine compared with control cells. These values were normalized against nearby myofibrils and we assessed differences between average values using student's t-test.: *: $P \leq 0.05$;

**: $P \leq 0.01$)

Figure 13: 1P (A) and 2P (B) myosin intensity in single cells treated with Y-27632 compared with control cells. These values were normalized against nearby myofibrils and we assessed differences between average values using student's t-test.: **: $P \leq 0.01$)

Figure 14: 1P (A) and 2P (B) myosin intensity in single cells treated with ML-7 compared with control cells. These values were normalized against nearby myofibrils and we assessed differences between average values using student's t-test.: **: $P \leq 0.01$)

Tables:

Table 1

A:

Treatment	Number of cells	Number of half-bivalent pairs			
		Total	Stopped	Slowed	No change
Staurosporine	19	37	11	20	6

B:

Staurosporine		Staurosporine + CalA	
Effect	Number of half- bivalent pairs	No change	Accelerated
Slowed or stopped	13	13	0

Table 2

Treatment	Number of cells	Number of half-bivalent pairs			
		Total	Stopped	Slowed	No change
BIM	8	16	1	2	13

Table 3

A:

Treatment	Number of cells	Number of half-bivalent pairs			
		Total	Stopped	Slowed	No change
Y-27632	7	14	1	10	3

B:

Y-27632		Y-27632+CalA	
Effect	Total # of half bivalent pairs	No change	Accelerated
No change	4	2	2
Slowed or stopped	8	0	8

Table 4

A:

Treatment	Number of cells	Number of half-bivalent pairs				
		Total	Stopped	Slowed	No change	Accelerated
ML-7	13	26	2	16	6	2

B:

ML-7		ML-7+CalA	
Effect	Total # of half bivalent pairs	No change	Accelerated
No change	1	1	0
Slowed or stopped	11	0	11

Table 5

A:

Treatment	Number of cells	Number of half-bivalent pairs followed			
		Total	Stopped	Slowed	No change
ML-7 +Y-27632	10	20	3	11	6

B:

Y-27632+ML-7		Y-27632+ML-7+CalA	
Effect	Total # of half bivalent pairs	No change	Accelerated
No change	6	6	0
Slowed or stopped	13	0	13

A

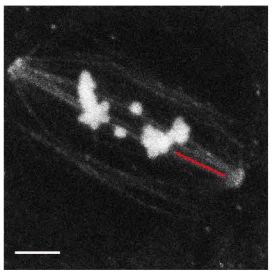

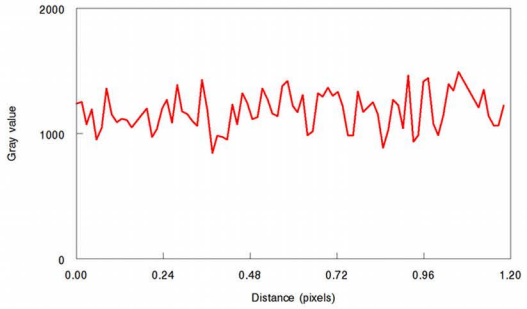
2000
1000
0
Gray value
0.00
0.24
0.48
0.72
0.96
1.20
Distance (pixels)

B

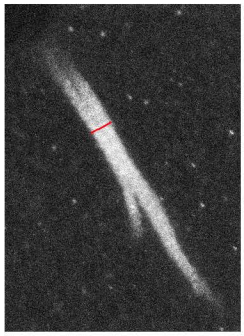

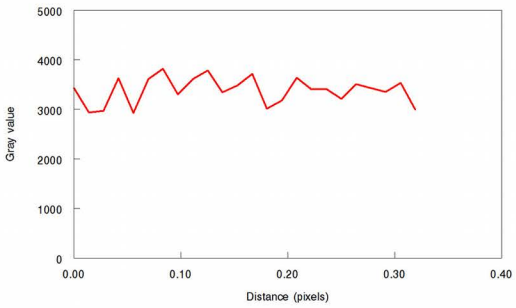
5000
4000
3000
2000
1000
0
Gray value
0.00
0.10
0.20
0.30
0.40
Distance (pixels)

Figure 1

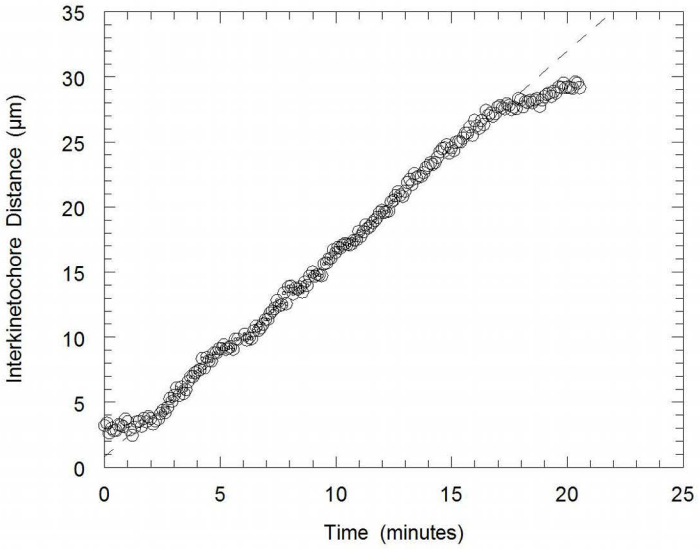
Interkinetochore Distance (µm)
35
30
25
20
15
10
5
0
0
5
10
15
20
25
Time (minutes)

Figure 2

A

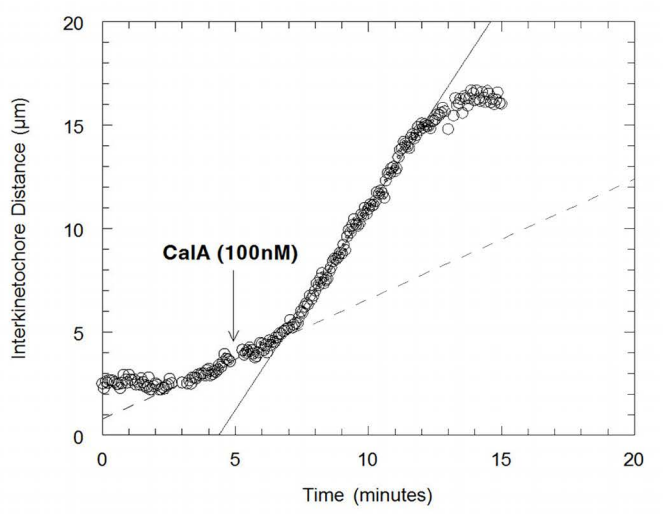
Interkinetochore Distance (µm)
Time (minutes)
CalA (100nM)
0
5
10
15
20

B

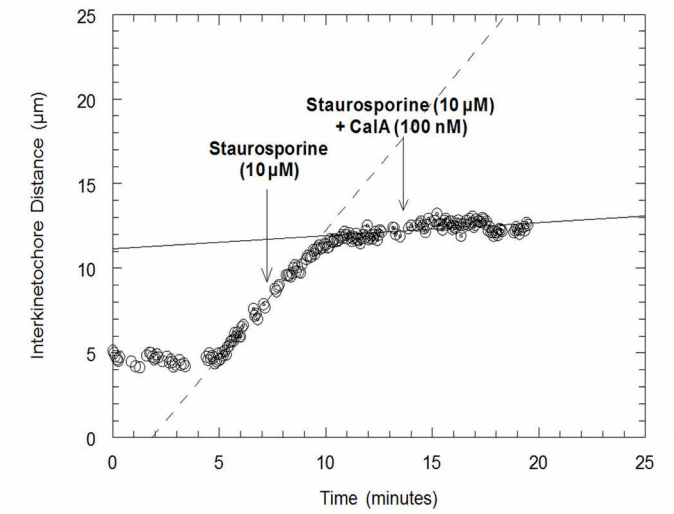
Interkinetochore Distance (µm)
Time (minutes)
Staurosporine (10 µM)
+ CalA (100 nM)
Staurosporine
(10 µM)
0
5
10
15
20
25

C

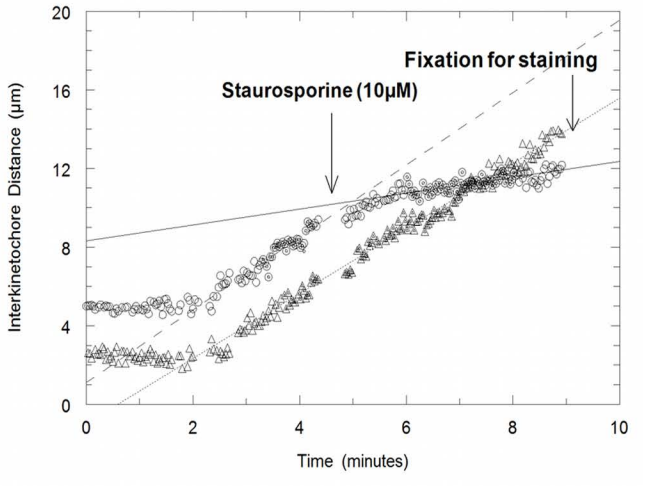
Interkinetochore Distance (µm)
Time (minutes)
Fixation for staining
Staurosporine (10µM)
0
2
4
6
8
10
12
16
20

Figure 3

A

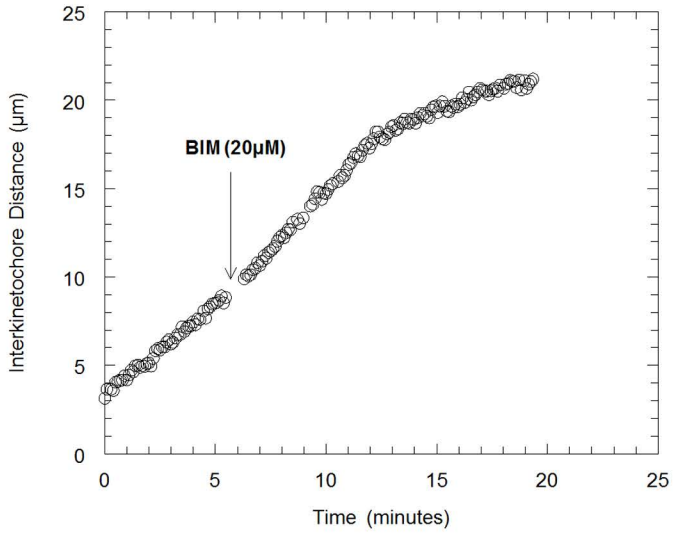
Interkinetochore Distance (µm)
BIM (20µM)
Time (minutes)
0
5
10
15
20
25

B

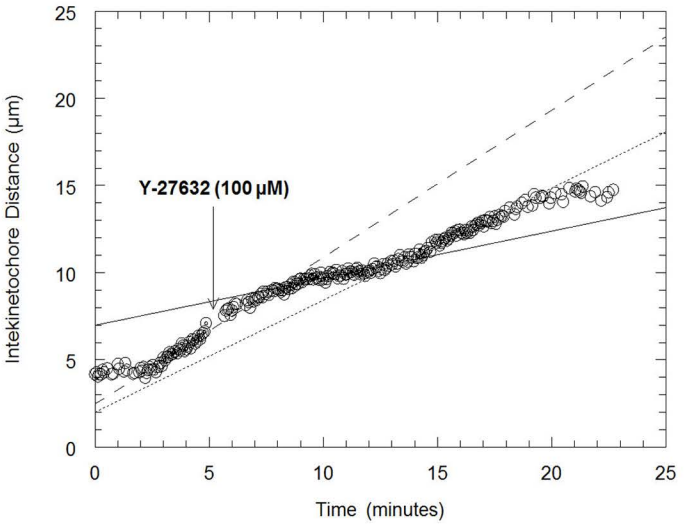
Intekinetochore Distance (µm)
Y-27632 (100 µM)
Time (minutes)
0
5
10
15
20
25

Figure 4

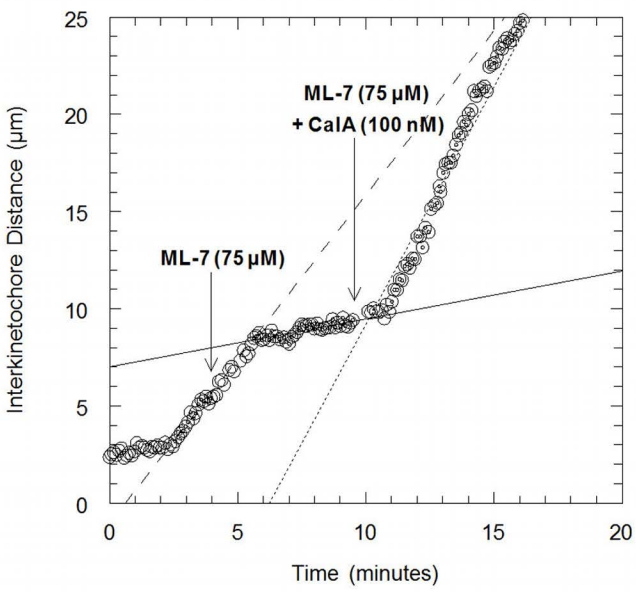
ML-7 (75 µM)
+ CalA (100 nM)
ML-7 (75 µM)
Interkinetochore Distance (µm)
Time (minutes)
0
5
10
15
20
25

Figure 5

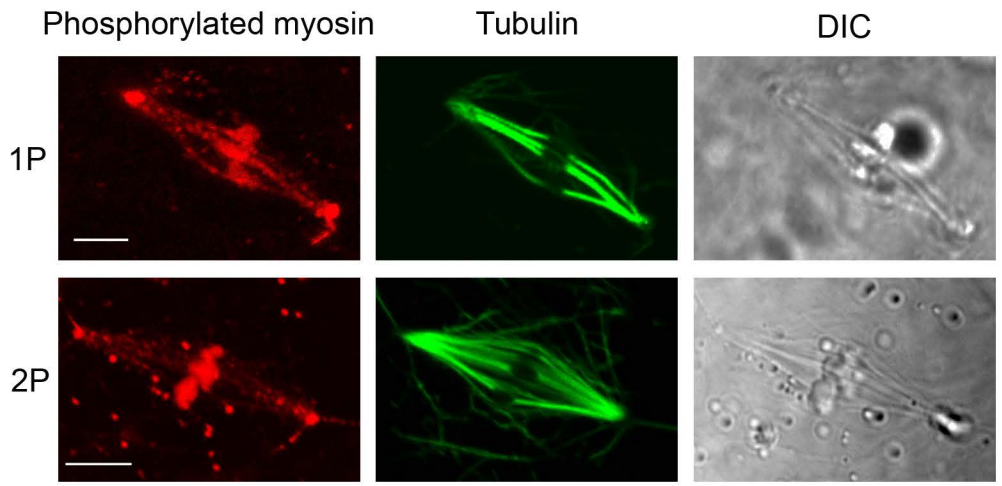

Figure 6

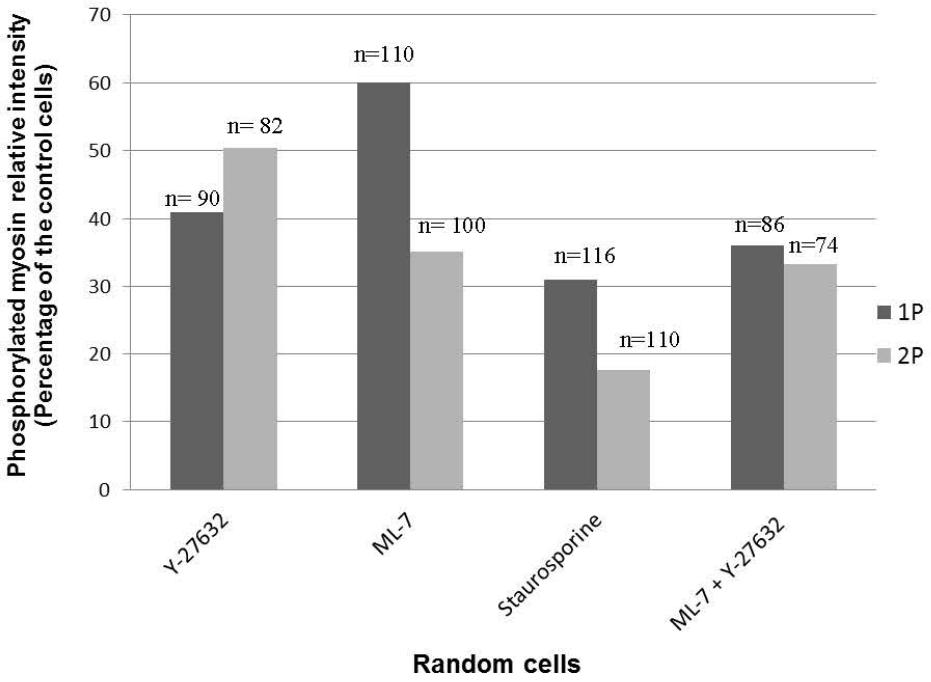
Phosphorylated myosin relative intensity (Percentage of the control cells)
70
60
50
40
30
20
10
0
n= 90
n= 82
n=110
n= 100
n=116
n=110
n=86
n=74
1P
2P
Y-27632
ML-7
Staurosporine
ML-7 + Y-27632
Random cells

Figure 7

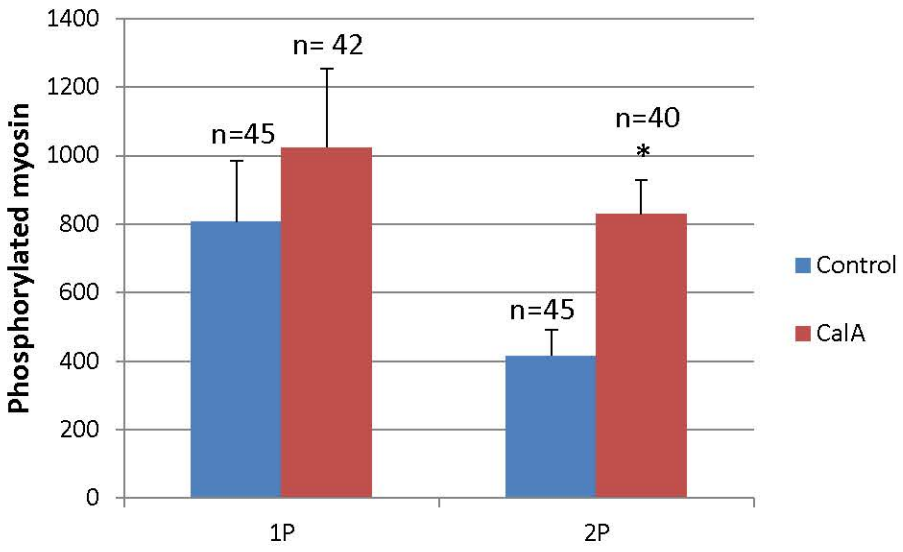
1400
1200
1000
800
600
400
200
0
Phosphorylated myosin
n= 42
n=45
n=40
*
n=45
1P
2P
Control
CalA

Figure 8

A:

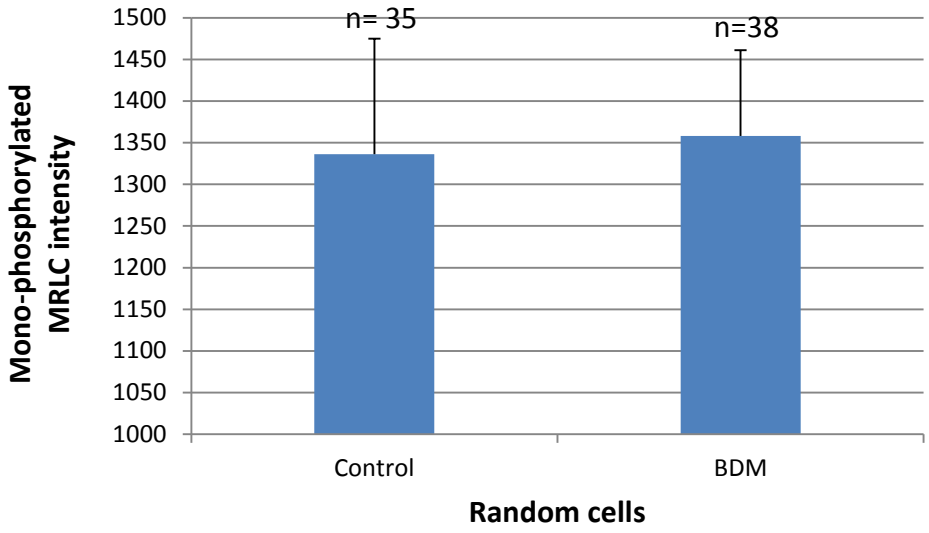
Mono-phosphorylated MRLC intensity
1500
1450
1400
1350
1300
1250
1200
1150
1100
1050
1000
n= 35
n=38
Control
BDM
Random cells

B:

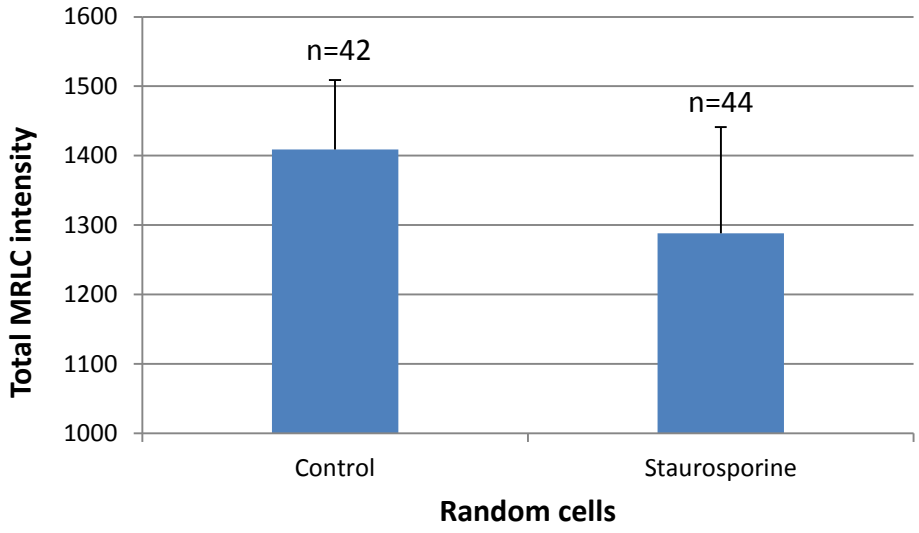
Total MRLC intensity
1600
1500
1400
1300
1200
1100
1000
n=42
n=44
Control
Staurosporine
Random cells

Figure 9

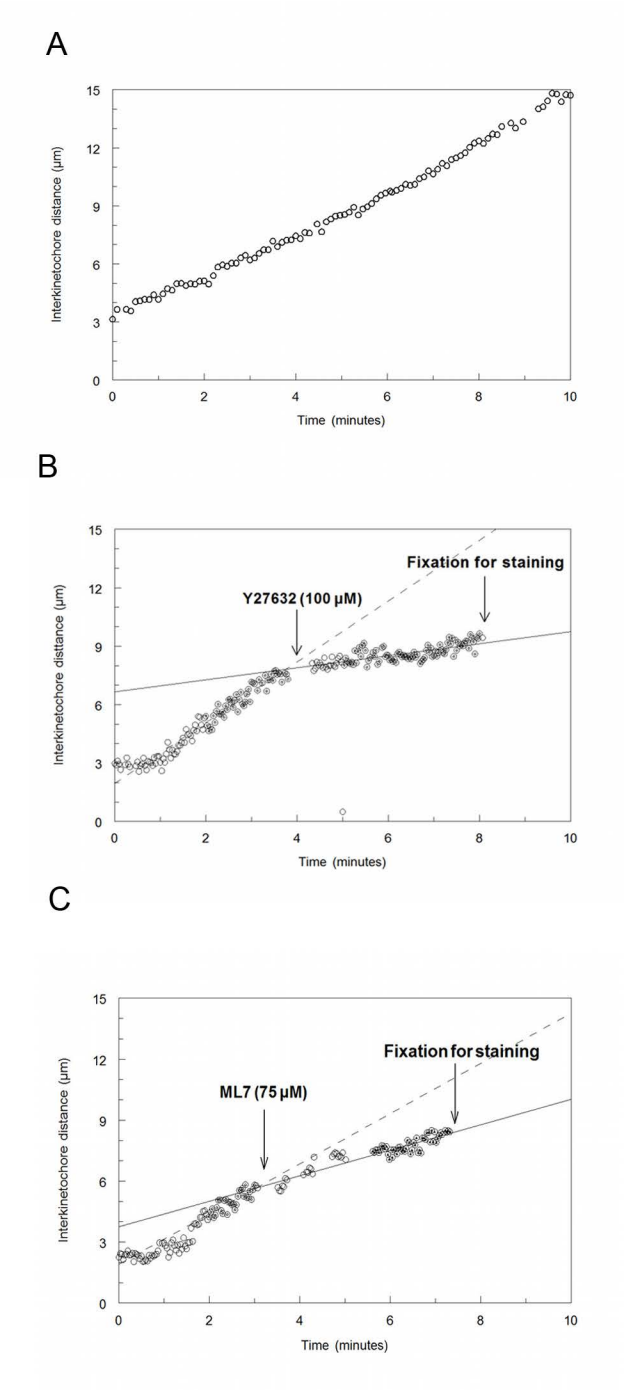
A
Interkinetochore distance (µm)
Time (minutes)
B
Interkinetochore distance (µm)
Y27632 (100 µM)
Fixation for staining
Time (minutes)
C
Interkinetochore distance (µm)
ML7 (75 µM)
Fixation for staining
Time (minutes)

Figure 10

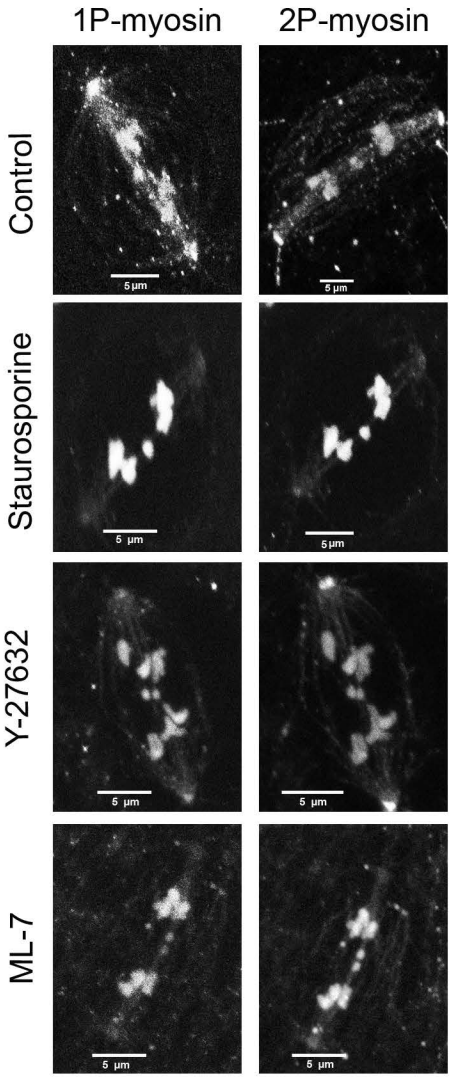

Figure 11

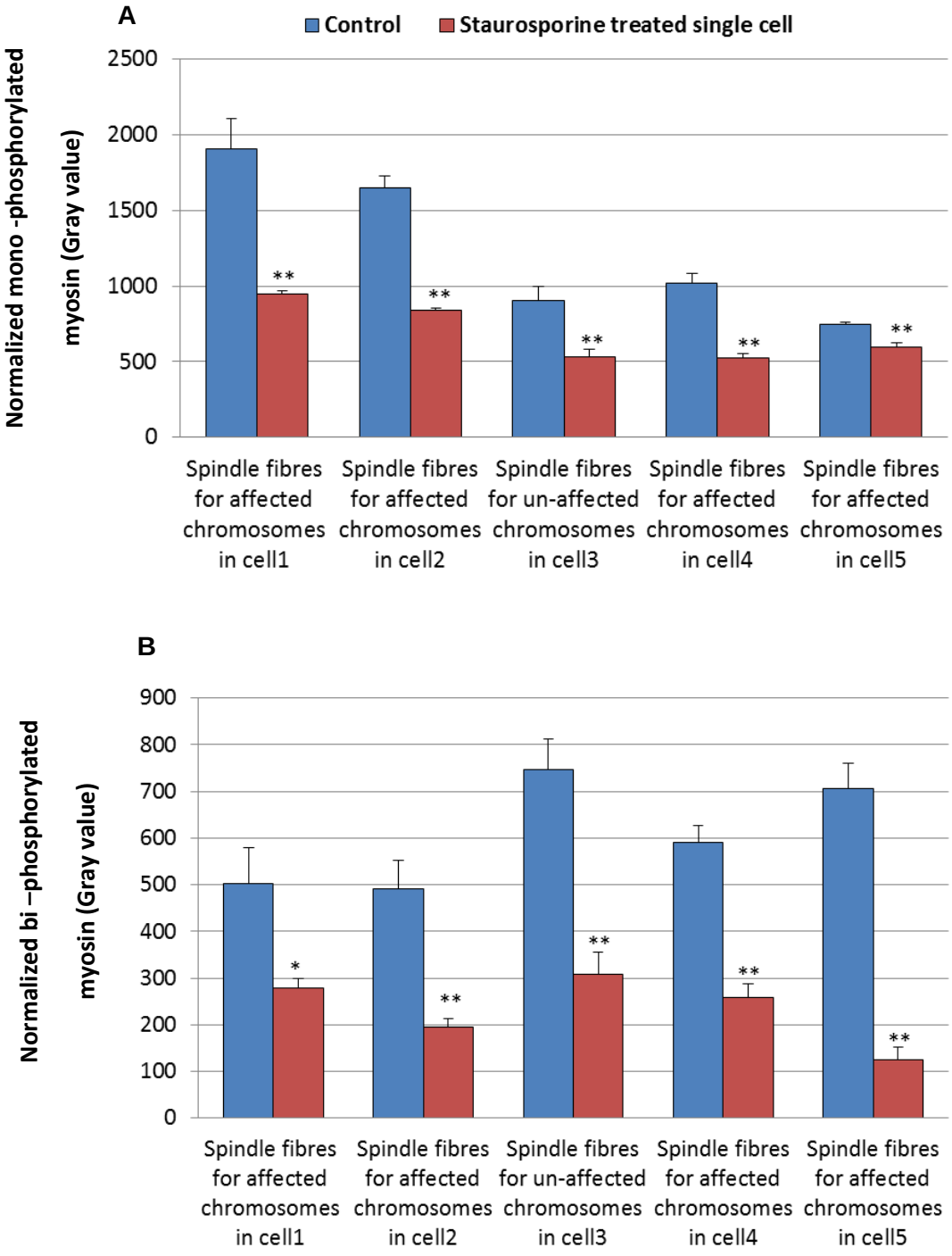
A
Control
Staurosporine treated single cell
Normalized mono -phosphorylated myosin (Gray value)
2500
2000
1500
1000
500
0
**
**
**
**
**
Spindle fibres for affected chromosomes in cell1
Spindle fibres for affected chromosomes in cell2
Spindle fibres for un-affected chromosomes in cell3
Spindle fibres for affected chromosomes in cell4
Spindle fibres for affected chromosomes in cell5
B
Normalized bi –phosphorylated myosin (Gray value)
900
800
700
600
500
400
300
200
100
0
*
**
**
**
**
Spindle fibres for affected chromosomes in cell1
Spindle fibres for affected chromosomes in cell2
Spindle fibres for un-affected chromosomes in cell3
Spindle fibres for affected chromosomes in cell4
Spindle fibres for affected chromosomes in cell5

Figure 12

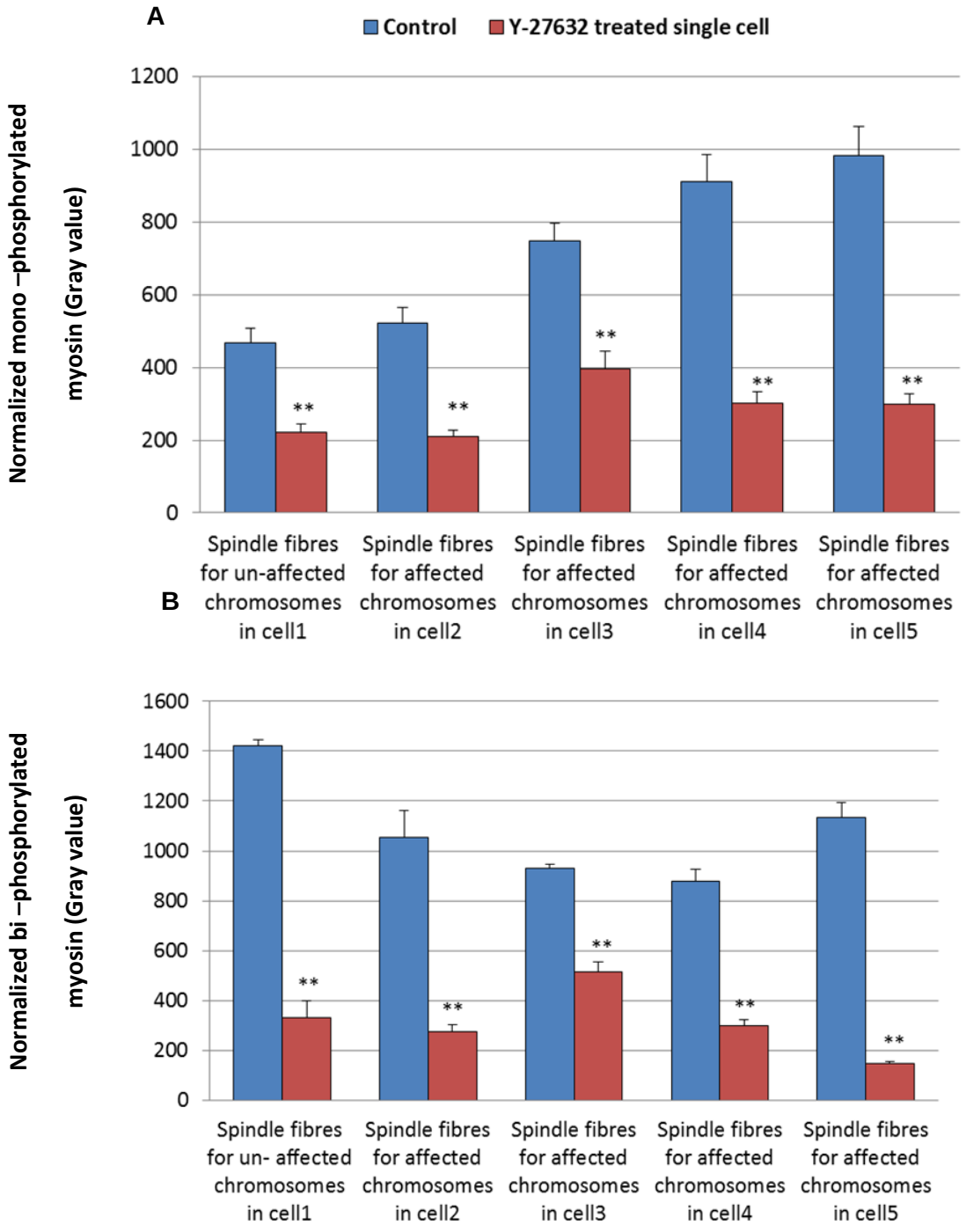
A
Control
Y-27632 treated single cell
Normalized mono –phosphorylated myosin (Gray value)
1200
1000
800
600
400
200
0
**
Spindle fibres for un-affected chromosomes in cell1
Spindle fibres for affected chromosomes in cell2
Spindle fibres for affected chromosomes in cell3
Spindle fibres for affected chromosomes in cell4
Spindle fibres for affected chromosomes in cell5
B
Normalized bi –phosphorylated myosin (Gray value)
1600
1400
1200
1000
800
600
400
200
0
Spindle fibres for un- affected chromosomes in cell1
Spindle fibres for affected chromosomes in cell2
Spindle fibres for affected chromosomes in cell3
Spindle fibres for affected chromosomes in cell4
Spindle fibres for affected chromosomes in cell5

Figure 13

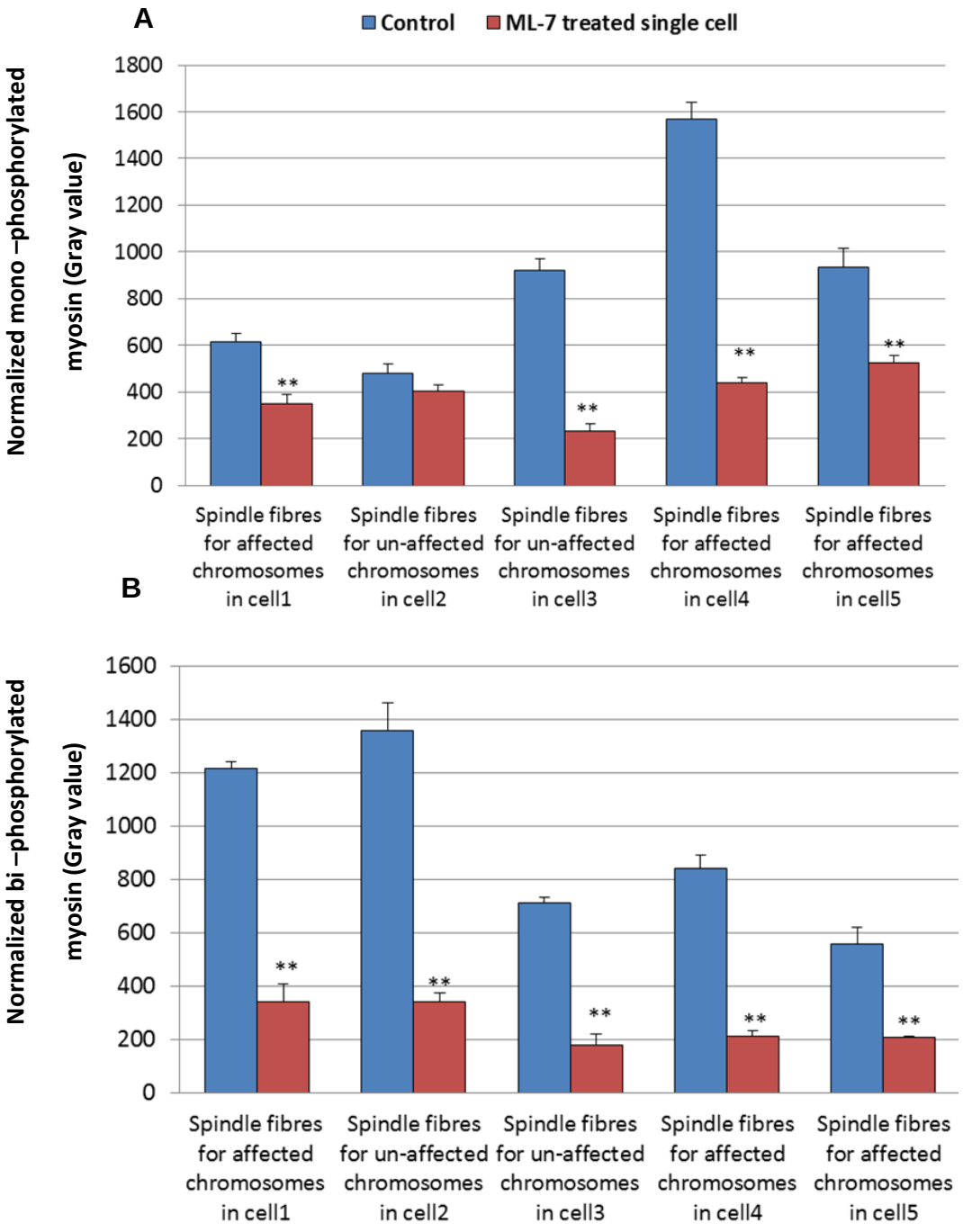
A
Control
ML-7 treated single cell
Normalized mono –phosphorylated myosin (Gray value)
1800
1600
1400
1200
1000
800
600
400
200
0
**
Spindle fibres for affected chromosomes in cell1
Spindle fibres for un-affected chromosomes in cell2
Spindle fibres for un-affected chromosomes in cell3
Spindle fibres for affected chromosomes in cell4
Spindle fibres for affected chromosomes in cell5
B
Normalized bi –phosphorylated myosin (Gray value)
1600
1400
1200
1000
800
600
400
200
0
**
Spindle fibres for affected chromosomes in cell1
Spindle fibres for un-affected chromosomes in cell2
Spindle fibres for un-affected chromosomes in cell3
Spindle fibres for affected chromosomes in cell4
Spindle fibres for affected chromosomes in cell5

Figure 14